Vision Research 218 (2024) 108380

Contents lists available at ScienceDirect

Vision Research

journal homepage: www.elsevier.com/locate/visres

Biological motion perception in the theoretical framework of perceptual decision-making: An event-related potential study

Osman Cagri Oguz [a,b,*], Berfin Aydin [b], Burcu A. Urgen [a,b,c]

[a] Department of Psychology, Bilkent University, Ankara 06800, Turkey
[b] Department of Neuroscience, Bilkent University, Ankara 06800, Turkey
[c] Aysel Sabuncu Brain Research Center and National Magnetic Resonance Research Center (UMRAM), Bilkent University, Ankara 06800, Turkey

ARTICLE INFO

Keywords:
Visual perception
Biological motion
Perceptual decision-making
EEG
CPP

ABSTRACT

Biological motion perception plays a critical role in various decisions in daily life. Failure to decide accordingly in such a perceptual task could have life-threatening consequences. Neurophysiology and computational modeling studies suggest two processes mediating perceptual decision-making. One of these signals is associated with the accumulation of sensory evidence and the other with response selection. Recent EEG studies with humans have introduced an event-related potential called Centroparietal Positive Potential (CPP) as a neural marker aligned with the sensory evidence accumulation while effectively distinguishing it from motor-related lateralized readiness potential (LRP). The present study aims to investigate the neural mechanisms of biological motion perception in the framework of perceptual decision-making, which has been overlooked before. More specifically, we examine whether CPP would track the coherence of the biological motion stimuli and could be distinguished from the LRP signal. We recorded EEG from human participants while they performed a direction discrimination task of a point-light walker stimulus embedded in various levels of noise. Our behavioral findings revealed shorter reaction times and reduced miss rates as the coherence of the stimuli increased. In addition, CPP tracked the coherence of the biological motion stimuli with a tendency to reach a common level during the response, albeit with a later onset than the previously reported results in random-dot motion paradigms. Furthermore, CPP was distinguished from the LRP signal based on its temporal profile. Overall, our results suggest that the mechanisms underlying perceptual decision-making generalize to more complex and socially significant stimuli like biological motion.

1. Introduction

One of the fundamental roles of the human visual system lies in its capacity to perceive and discern animate movements within its surroundings. Notably, perception of biological motion influences various judgments, including the recognition of living entities, agency attribution, responding to and interacting with those agents in the environment, and shaping broader social cognition. The human visual system remarkably and efficiently executes this function (Blake & Shiffrar, 2007; Pavlova, 2012; Rutherford & Kuhlmeier, 2013; Johnson & Shiffrar, 2013; Brooks et al., 2007). To illustrate, envision a scenario of driving a car when suddenly confronted with a pedestrian or a dog. Our visual system promptly detects the motion characteristic of a living being, which results in an immediate deceleration or halt. Without this essential ability, the consequences could become life-threatening. This highlights the significance of delving into biological motion perception within the realm of perceptual decision-making.

Perceptual decision-making and its neural mechanisms have been widely researched in systems and cognitive neuroscience, employing a range of techniques from invasive neurophysiology in non-human primates to non-invasive neuroimaging in humans and computational modeling. The random-dot motion paradigm has been utilized as a prominent tool, involving displays of moving dots with a subset coherently moving in a specific direction (signal) while others move randomly (noise) (Newsome et al.,1989). By adjusting the proportion of signal dots, researchers can control the stimulus coherence and simulate real-world scenarios where information is often ambiguous and noisy. Historically, this paradigm has been primarily used with non-human primates while recording the neural firing rate in different brain areas to reveal the underlying mechanisms of perceptual decision-making

* Corresponding author.
E-mail addresses: cagri.oguz@bilkent.edu.tr (O.C. Oguz), burcu.urgen@bilkent.edu.tr (B.A. Urgen).

https://doi.org/10.1016/j.visres.2024.108380
Received 28 September 2023; Received in revised form 6 March 2024; Accepted 6 March 2024
Available online 12 March 2024

(Horwitz & Newsome, 1999; Kim & Shadlen, 1999; Shadlen & Newsome, 1996). An influential neurophysiology study by Shadlen & Newsome (2001) examined neural firing rates in monkeys time-locked to the stimulus and response onset. The findings demonstrated a correlation between increased stimulus coherence and neural firing rates in the lateral intraparietal area (LIP), contrasting with findings from the middle temporal area (MT), a brain region typically associated with motion perception. Moreover, researchers observed that activity of LIP neurons reached a uniform level during the response, irrespective of stimulus coherence. Therefore, it has been suggested that neurons play a critical role in perceptual decision-making (Shadlen & Newsome, 2001; Gold & Shadlen, 2007). These insights have been integrated into various computational models, with one prominent example being the drift–diffusion model (Smith & Ratcliff, 2004; Ratcliff & McKoon, 2008). The model consists of two main components: accumulation of sensory evidence and decision boundary. Essentially, the drift–diffusion model proposes that during perceptual decision-making, our sensory system initially collects and accumulates evidence over time, ultimately surpassing a predetermined threshold for the decision to be reached, namely the decision boundary (Bach et al., 2011). Importantly, these processes resonate in the neural firing rates observed in the LIP.

On the other hand, when investigating perceptual decision-making in humans, researchers predominantly utilized non-invasive techniques, including high temporal resolution EEG (Kelly & O'Connell, 2013, 2015; Twomey et al., 2015). Event-related potentials (ERPs), coupled with behavioral measures are key dependent variables in these studies. The seminal work by Kelly and O'Connell (2013) manipulated the coherence level of random dot stimuli for a direction task, akin to previous non-human primate research, while the target motion stimuli were preceded by the scrambled dots. The results demonstrated that stimuli coherence increase is associated with reduced miss rates and faster mean response times. More importantly, the study revealed an ERP, Centro-Parietal Positivity (CPP), characterized by a positive distribution over centroparietal electrodes and emerging between 200 and 800 ms following the target presentation. The temporal and signal profile of CPP revealed a shorter peak latency and a larger amplitude as the coherence increased. Moreover, the response-locked analysis indicated that average CPP signals across different coherence levels converged at the response time. Numerous other studies have demonstrated complementary outcomes to CPP-related work on perceptual decision-making, encompassing various tasks and stimuli on a variety of sensory domains; namely visual (Philiastides et al., 2006), auditory (Kaiser et al., 2006), and somatosensory (Herding et al., 2019). Collectively, these studies suggest that CPP systematically builds up depending on evidence strength, irrespective of the sensory modalities, the manipulations targeting signal-to-noise ratio of the targets (e.g., intensity or volume changes), or the motor demands of the task including button presses (O'Connell et al., 2012; Kelly & O'Connell, 2015). In other words, CPP is thought to reflect both the sensory evidence accumulation process and the decision boundary postulated by the drift–diffusion model (Kelly & O'Connell, 2013).

Another event-related potential investigated within perceptual decision-making studies, particularly when there is a motor component for response reporting, is Lateralized Readiness Potential (LRP). This potential, whose source is considered to be within the primary motor cortex (De Jong et al., 1988), is regarded as reflecting the unimanual motor preparation process, demonstrating a negative-going potential contralateral to the hand being utilized for the response. Notably, it has been found that even in the absence of explicit motor response, preparatory activation is sufficient to evoke this potential (Smulders & Miller, 2012). In a study by Kelly & O'Connell (2013), it has been suggested that LRP, indexing the motor preparation phase, temporally follows CPP, indexing supramodal sensory evidence accumulation (but see Lui et al., 2021).

To the best of our knowledge, biological motion perception has yet to be explicitly studied within the theoretical framework of perceptual decision-making, holding promise for substantial insights. Point-light displays (PLDs) have emerged as fundamental stimuli for investigating biological motion perception, consisting of dots representing the joints of a moving actor (Johansson, 1973). Although these displays lack some fine details typically present in the natural motion of biological organisms, such as color, texture, and depth information, they still offer a valuable tool for studying the visual system's ability to detect and process animate movement (Johansson, 1976; Blake & Shiffrar, 2007). PLDs allow the brain to integrate and process the motion trajectories of individual dots embedded in the displays and to represent the structure with coherent forms (i.e. the human body). There is a large literature investigating the contributions of low-level features, such as global form and local motion information to biological motion perception (Chang & Troje, 2008, Troje & Westhoff, 2006, Casile & Giese, 2005, Thornton, 2006). In this respect, exploring the information processing stages of biological motion perception from sensory evidence accumulation to bound dynamics, provides a valuable opportunity to integrate the two fields. This endeavor, by offering a close inspection of the temporally evolving signal, holds a promise for enhancing our understanding of biological motion perception and its underlying mechanisms. Accordingly, the present study is dedicated to investigating the neural and temporal dynamics of perceptual decision-making processes by employing a task featuring PLDs.

Furthermore, the limitations of the perceptual decision-making literature can be effectively addressed by introducing PLDs. Particularly, widely employed random dot kinematograms (RDKs) offer limited complexity and lack social significance. Apart from the works utilizing RDKs, studies in the visual domain have predominantly employed relatively simple or static stimuli; including gabor patches, varying-sized circles, arrow sequences, face versus car images (Heekeren et al., 2008; de Lange et al., 2010; Cheadle et al., 2014; Gorea et al., 2014). However, the extent to which underlying temporal dynamics of perceptual decision-making revealed for these simpler stimuli generalize to more complex and social situations involving motion, such as biological motion, remains unknown. In this respect, point-light displays are promising to overcome these limitations through inherently complex form and motion interplay and by presenting socially meaningful and ecologically better non-static stimuli.

In light of these, the present study investigated the core decision-making processes by embedding the PLDs in different noise levels. Given the evidence obtained from diverse stimuli and modalities as previously outlined, one could anticipate that the core mechanisms underlying perceptual decision-making extend to biological motion processing. To this end, we recorded behavior and EEG activity during PLD walker direction discrimination task consisting of four conditions in which the amount of randomly moving dots is varied to manipulate the coherency of the target stimuli. We hypothesized that the increases in mean reaction time and miss rate would inversely follow the changes to that of the coherence. Regarding ERPs, we expected that CPP would track the coherence level of the biological motion stimuli. However, we expected a potentially later onset for CPP than in previous studies since the perception of biological motion may require more time to process than random dot motion stimuli due to its complexity. In addition, we also examined LRP as an index of motor preparation (Gratton et al.,1988) and aimed to distinguish it from CPP, following the previous work (Kelly & O'Connell, 2013).

2. Methods and materials

2.1. Participants

A total of 16 participants (8 female, mean age = 23.18, age range [18 40]) with normal or corrected-to-normal vision participated in the study. None of the participants had a neurological or psychiatric disorder and were using any psychiatric medication. The Human Research Ethics Board of Bilkent University approved the study. Participants were

informed about the study procedures and signed a consent form before participation. In the pre-screening form, all participants reported at least 6 h of sleep to avoid confounding effects on the EEG signal and performance.

2.2. Stimuli, experimental design, and procedure

The experiment utilized point-light displays for the biological motion stimuli to investigate human perceptual decision-making with EEG, renowned for its efficacy in capturing biological motion DYNAMICS. The biological motion stimuli in the task portrayed a human walking action, featuring 13 dots representing the joints on both sides of the body and the head, with an overall size of 6.5 degrees. The walking direction could be either to the right or left while the stimuli were displayed from the side view of the corresponding direction. The gait cycle for the walking phase lasts around 700 ms. The participants were asked to report the direction as soon as they detected the walking human while the target walking stimuli were displayed, which can last for 2 s at most and correspond to approximately 3 full gait cycles. The motion targets appear as forward walking towards left or right on a treadmill. The starting point in the gait cycle was randomized in each trial.

For the scrambled motion stimuli, the motion vector of the dots mirrored that of the meaningful biological motion stimuli. However, instead of moving in a coherent direction to simulate human walking, the dots appeared to move randomly since their starting coordinates were randomized. Similar to the biological motion stimuli, varying degrees of noise dots were introduced into the scrambled motion displays. To maintain uniformity within each trial, the number of noise dots introduced for the scrambled motion stimuli matched those introduced for the subsequent biomotion stimuli.

For coherence manipulation, the biological motion stimuli were embedded in different levels of noise. Specifically, different quantities of dots were introduced into the display, effectively determining the trial's noise level. These noise levels were determined through a pilot study, ensuring that manipulation of difficulty spanned four discernible levels. As a result, manipulation of difficulty was accomplished across four distinct noise levels: 10, 20, 35, 55.

Each of the four noise levels featured 120 trials, resulting in 480 trials in total for the whole experiment. The experiment was structured into four blocks, each consisting of 120 trials of varying levels of noisy stimuli. The counterbalancing mechanism ensured trial uniformity, encompassing both the direction of biological motion stimuli and the noise levels.

A preliminary practice task was administered for participants' familiarization with the task. Participants were instructed to fixate on the center - where the fixation point was displayed - while performing the task. The screen was viewed at a 57 cm distance. Additionally, participants were also explicitly instructed to report the walking direction upon recognizing a human figure using bimanual key presses during the target interval. Each trial started with the presentation of a fixation point for 1 s at the trial's onset, placed at the center of the screen to direct the participant's attention to the designated area. Then, it was followed by the scrambled motion display. The scrambled motion stimuli were displayed at varying durations (3, 5, or 8 secs) to prevent the predictability of the target stimulus. After the scrambled motion, the target biological motion stimulus was displayed for a maximum of 2 s (See Fig. 1). The transition from scrambled to biological motion stimuli was executed seamlessly to eliminate potential immediate visual evoked potentials in the EEG data.

2.3. Data collection and analysis

2.3.1. Behavioral

The mean response time and miss rate for the direction discrimination task were recorded and analyzed for each noise level. Response time, which is defined as the period that spans the onset of the biological motion stimulus until the participant gives a response, was taken for the correct trials. The miss rate indicates the proportion of trials where participants failed to respond during the target stimulus presentation. This measure provides information on the participant's ability to detect the target and respond on time. One-way repeated measures analysis of variance (ANOVA) was applied to examine how different noise levels affected the mean response time and miss rate. Our hypothesis posited that as noise levels increased, response time and miss rates would also increase.

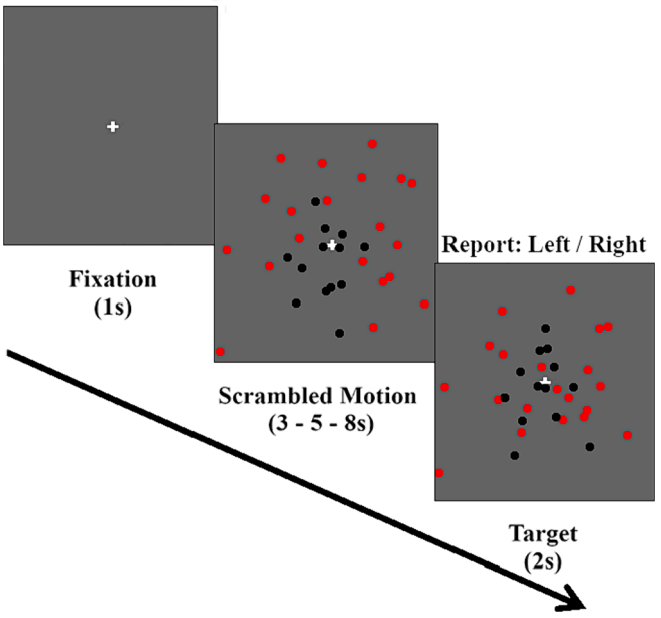

Fig. 1. Experimental Setup. The example trial is illustrated with noise level 20 and the walking direction to the left. The red dots are depicted to highlight the noisy dots and all of the dots are in larger sizes than the actual stimuli for display purposes.

2.3.2. EEG Recording and Pre-processing

64-channel EEG (Brain Products, GmbH, Germany) was recorded at 512 Hz using sintered Ag/AgCl passive electrodes whose placements were according to the international 10/20 system. The electrode AFz was used as ground and FCz was used as reference. Electrode offset was kept below 25 k ohm. Pre-processing was done using Matlab and the EEGLAB toolbox (Delorme & Makeig, 2004). The analysis focused on 63 EEG channels after excluding the ECG channel. Data underwent a 1 Hz high-pass and 50 Hz low-pass filter, followed by re-referencing to the average of all electrodes. Eye-related components were removed using Independent Component Analysis (ICA), specifically by the binica algorithm. Data were then epoched for stimulus-locked and response-locked analysis. Epoch time intervals were determined based on the mean response times instead of minimum response times for accurate trials for each participant due to the insufficiency of the latter to capture the entire decision process. The minimum mean response time among all participants was approximately 830 ms. Thus, our analyses incorporated 800 ms post-target and pre-response.

For the stimulus-locked analysis, data from 200 ms before to 800 ms after the target were included, with baseline correction applied using the interval [-200, 0]. The response-locked analysis covered 800 ms before to 100 ms after the response, without baseline correction. Epochs containing artifacts were removed through semi-automated methods in EEGLAB, which identified improbable and abnormally distributed signals. Following EEGLAB's pre-processing, event-related potentials were computed using ERPLAB (Lopez-Calderon & Luck, 2014).

2.3.3. ERP analysis

We examined the effect of noise level on two event-related potentials (ERPs), namely centro-parietal positivity (CPP) and lateralized readiness potential (LRP), through both stimulus-locked and response-locked analysis.

CPP, typically measured by averaging the amplitude of the electrodes CPz and its bilateral neighboring electrodes CP1 and CP2 (Kelly & O'Connell, 2013; 2015), was computed accordingly. In stimulus-locked analysis, a preliminary inspection of grand average ERP waveforms in those channels revealed the rise having approximately 350 ms onset. Hence, we analyzed [350 800] interval for stimulus-locked analysis. For response-locked analysis, we considered the [-450 0] interval to maintain consistent duration between both analyses. We employed one-way ANOVA on CPP amplitudes with the noise level as the main factor for both analyses. Pairwise comparisons were subsequently performed among the four noise levels. To explore further, we employed a more conservative approach utilizing false discovery rate (FDR) correction with the channels specified above and the time points included (Fields, 2017; Fields & Kuperberg, 2020). For the stimulus-locked analysis, the time points from the stimulus onset to 800 ms post-stimulus; while for the response-locked analysis, the time points from 800 ms pre-response to the response onset were included. Scalp maps were also generated to visualize signal distribution across the entire brain during the epoch intervals. For LRP analysis, a measure of unimanual response preparation, a pair of electrodes from central and frontocentral regions in each hemisphere (C3-C4, and FC3-FC4) were included, in line with the literature (Eimer, 1998; Kelly & O'Connell, 2013). LRP for each trial was computed by subtracting the contralateral from ipsilateral channel activity with respect to the walking direction of the target stimuli in the trial. We initially utilized ANOVA with FDR correction including all time points following the stimulus or preceding the response onset. Following this, we also performed the analysis to include only FC3 and FC4 channels in the time interval approximately 100 ms later than the onset of CPP differentiation. Thus, in the latter analysis, the [450 800] interval for the stimulus-locked and the [-350 0] interval for the response-locked analysis were included. This analysis aimed to ascertain whether LRP temporally followed CPP, as suggested by Kelly and O'Connell (2013).

3. Results

3.1. Behavior

The results of the behavioral analysis demonstrated that the mean response time and miss rate followed a trend aligned with the experiment's difficulty level (see Fig. 2). The mean response time (Fig. 2, left) and miss rate (Fig. 2, right) increased as the noise level increased. The mean response time for different noise levels ranges from 1 to 1.4 s, while the miss rate ranges from 1 % to 25 %.

One-way ANOVA indicated a main effect of the noise level on the mean response time ($F[3,45] = 246.953$, $p < 0.001$, $\eta_p^2 = 0.943$), and all pairwise comparisons showed significant differences between the noise levels ($p < 0.001$ for each comparison, see Table 1). Similarly, a main effect of the noise level was found on the miss rate ($F[3,45] = 101.562$, $p < 0.001$, $\eta_p^2 = 0.871$). Additionally, pair-wise comparisons between noise levels on miss rate revealed significant results ($p < 0.005$), further providing support for the successful manipulation of difficulty in the experiment (see Table 1).

3.2. Centro-Parietal Positivity (CPP)

3.2.1. Stimulus-locked

To illustrate the effects of noise levels on CPP, we plotted the ERPs from stimulus onset to 800 ms post-stimulus. Complementing this, we generated scalp maps to visualize the general distribution of activity and its significance (See Fig. 3A). Initial inspection of the plot revealed that CPP waveforms align with the difficulty level of the target stimuli, displaying lower peak amplitudes and slower build-up rates as noise levels increase. The scalp maps further underscored the increased activity for conditions with lower noise levels, with a distribution concentrated on the centroparietal brain areas.

Employing one-way repeated-measures ANOVA on mean amplitudes from CPP channels (CP1, CP2, and CPz) during [350 800], a notable main effect of noise level was found ($F[3,6] = 196.615$, $p < 0.001$, $\eta_p^2 = 0.990$). Following this, to investigate the effect of our manipulation more thoroughly, we performed pair-wise t-tests. All of the comparisons revealed significant effects after the Bonferroni correction (see Table 2).

In an exploratory effort to comprehensively assess the CPP activation across the entire time range, we employed ANOVA with FDR correction for the CPP channels and encompassing time points from the stimulus onset to 800 ms post-stimulus. In this analysis, the correction was done considering the number of channels and the time interval included to reduce the effect of false positives and hence Type I errors (Fields, 2017).

Table 1
Pair-wise comparisons with corresponding t and p values for the miss rate (Miss) and mean reaction time (RT) across different noise levels.

Noise Level		t - Miss	p_{bonf} – Miss	t – RT	p_{bonf} – RT
10	**20**	−4.340	0.003	−8.800	<0.001
	35	−6.211	< 0.001	−17.058	<0.001
	55	−10.803	< 0.001	−25.936	<0.001
20	**35**	−5.854	< 0.001	−8.258	<0.001
	55	−12.837	< 0.001	−17.136	<0.001
35	**55**	−11.115	< 0.001	−8.878	<0.001

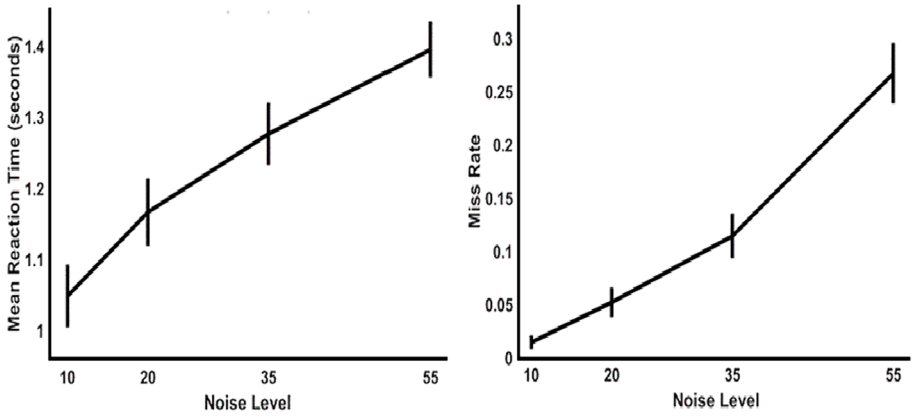

Fig. 2. Behavioral Results. The mean reaction time (left) and the miss rate (right) are given according to the corresponding noise levels of the biological motion stimulus.

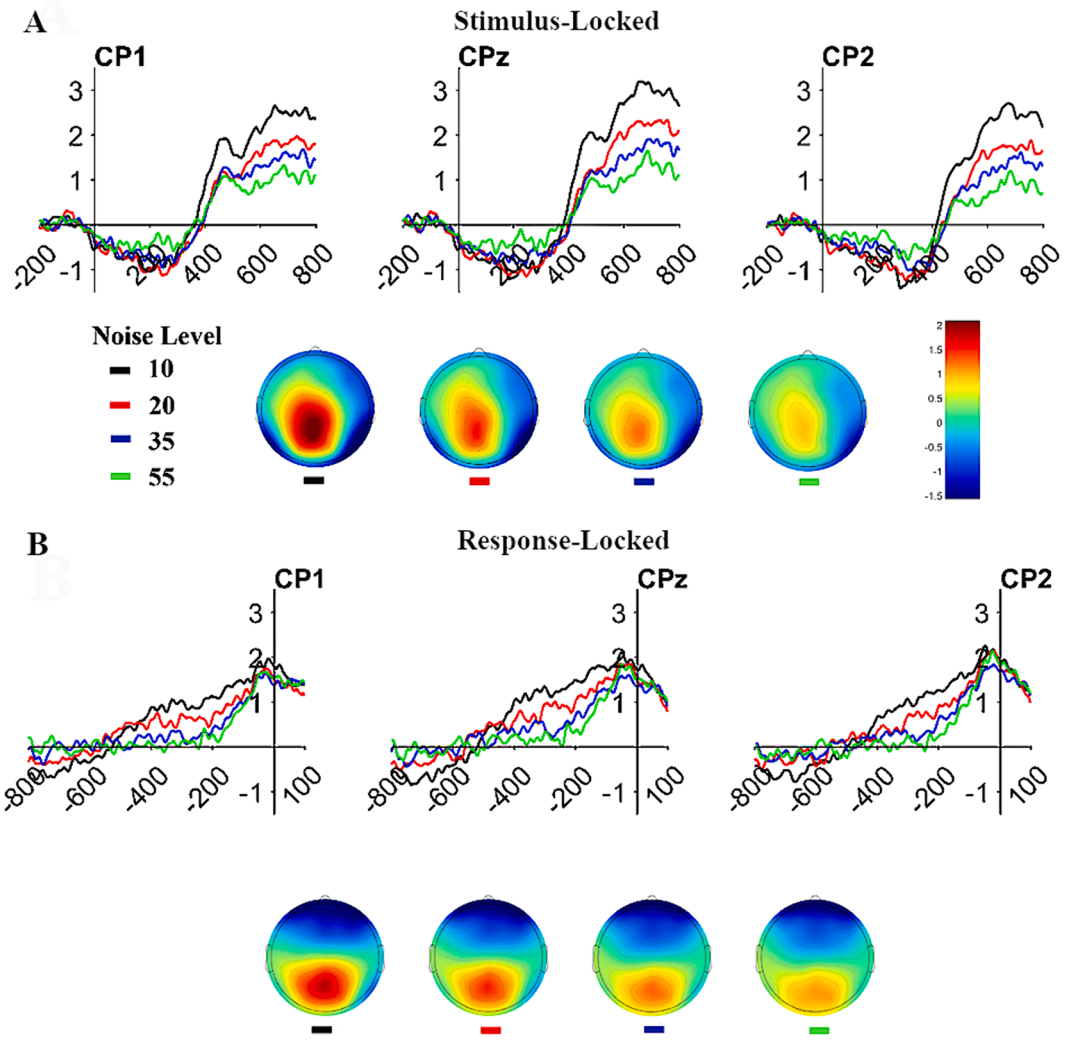

Fig. 3. CPP results. Stimulus-locked (A) and response-locked (B) waveform graphs demonstrating the amplitude over time for CP1, CP2, and CPZ channels along with the scalp maps.

Table 2
Pair-wise comparisons for the mean CPP amplitude in stimulus-locked analysis during [350 800] interval for different noise levels.

Noise Level		Mean Difference	t	Cohen's d	p_{bonf}
10	**20**	0.617	13.228	2.346	<0.001
	35	0.831	17.832	3.163	<0.001
	55	1.081	23.187	4.113	<0.001
20	**35**	0.215	4.605	0.817	0.022
	55	0.464	9.960	1.767	<0.001
35	**55**	0.250	5.355	0.950	0.010

This heightened level of conservatism enabled us to meticulously evaluate the significance of activations across CP1, CP2, and CPz, commencing right from the onset of the target stimulus. Remarkably, this analysis yielded a consistent pattern that mirrors the visual depiction of event-related potentials outlined above. Notably, the distinction in CPP responses based on varying noise levels began to emerge around 400 ms following the stimulus onset (see Supplementary Fig. 1). This investigation further confirmed the chosen time interval in epoching.

3.2.2. *Response-locked*

ERPs during [-800 100] for the response-locked analysis is illustrated along with the scalp maps (see Fig. 3B). The figure highlights the alignment of CPP waveforms with the task difficulty, showcasing heightened peak amplitudes and build-up rates in lower noise level conditions. In addition, scalp maps indicate more robust activity in less difficult conditions. Noteworthy is the tendency for activity across noise levels to converge at a certain level during the response (at 0 point for the response-locked analysis).

Consistent with the stimulus-locked analysis, we employed first a repeated-measures ANOVA on the mean amplitudes during the [-450 0] epoch interval. This analysis revealed a main effect of noise level ($F[3,6] = 276.680$, $p < 0.001$, $\eta p2 = 0.993$). Pair-wise tests between the noise levels also revealed significant differences between all comparisons except a marginally significant difference between noise levels 20 and 35 (See Table 3).

It is important to note that, as we have outlined above, the signals

Table 3
Pair-wise comparisons for the mean CPP activity in response-locked analysis during [-450 0] interval for different noise levels.

Noise Level		Mean Difference	t	Cohen's d	p_{bonf}
10	**20**	0.296	34.803	2.671	0.005
	35	0.597	16.651	5.385	0.022
	55	0.749	19.508	6.763	0.016
20	**35**	0.301	9.999	2.714	0.059
	55	0.453	14.475	4.091	0.028
35	**55**	0.153	18.276	1.378	0.018

from each electrode showed a tendency to reach a certain level regardless of the difficulty level during response execution (See Fig. 3B). This observation is also in line with the decision-making models that emphasize accumulation to bound dynamics. To further provide support for this trend, ANOVA with FDR correction is conducted on the [-800 0] time interval. The results of this analysis confirmed the trend with no main effect of noise on the activity observed in any of the CPP channels as the time approached the response onset (see Supplementary Fig. 2).

3.3. Lateralized readiness potential (LRP)

3.3.1. Stimulus-locked

To measure the lateralized readiness potential (LRP), we calculated the difference between contralateral and ipsilateral channels based on the target's walking direction. We included the electrodes from central and fronto-central sites as pairs (C3 and C4, FC3 and FC4) in line with the previous literature (Kelly and O'Connell, 2013). The LRP waveforms obtained from each pair during the epoched time interval for the stimulus-locked analysis were plotted in Fig. 4A. Employing ANOVA with FDR correction analysis on the mean activity during the period from the stimulus onset to 800 ms post-stimulus, we found that LRP activity did not exhibit the same alignment with task difficulty observed in CPP activity.

Following this, we performed a modified version of this analysis akin to the similar study done by Kelly & O'Connell (2013), where they detected a delayed LRP activity measured in frontocentral sites for approximately 100 to 150 ms in relation to CPP formation. Thus, we focused our analysis on the mean activity during the interval from 450 ms to 800 ms post-target, excluding C3 and C4 electrodes and narrowing it down to FC3 and FC4. Nevertheless, this analysis also failed to demonstrate a significant main effect of the noise level in the stimulus-locked data.

3.3.2. Response-locked

Similar to the stimulus-locked analysis, we plotted LRP waveforms for each electrode pair within the response-locked epoch (see Fig. 4B). Applying ANOVA with FDR correction analysis by considering the mean activity during the time interval from 800 ms pre-response to response onset, the alignment with the difficulty level was not observed as in the stimulus-locked analysis.

Interestingly, further modified analysis conducted on the response-locked data considering the mean activity during the period from 350 ms pre-response to response onset demonstrated a significant main effect of noise level, providing support for generalizing the previous findings in the literature ($F[3,45] = 3.3468$, $p = 0.03$). The discrepancy between stimulus-locked and response-locked results likely arises because of the stimulus-locked analysis not being well-suited to capture the response preparation interval, as compared to more insightful response-locked analysis.

4. Discussion

The present study aimed to investigate the neural dynamics of biological motion perception in the framework of perceptual decision-making, thereby integrating two lines of research. To achieve this, the experiment employed PLDs with varying degrees of noise dots to manipulate the difficulty level in the point-light walker direction discrimination task.

The behavioral results highlighted that overall task performance improved notably under low noise conditions. In essence, biological motion stimuli with heightened noise levels translated into delayed responses and an increased rate of misses, verifying our manipulation of task difficulty. On the other hand, investigating the electrophysiological results provided a more comprehensive overview of the neural underpinnings. Specifically, the amplitude of the CPP exhibited an upward trajectory and earlier peak under lower noise conditions. Furthermore,

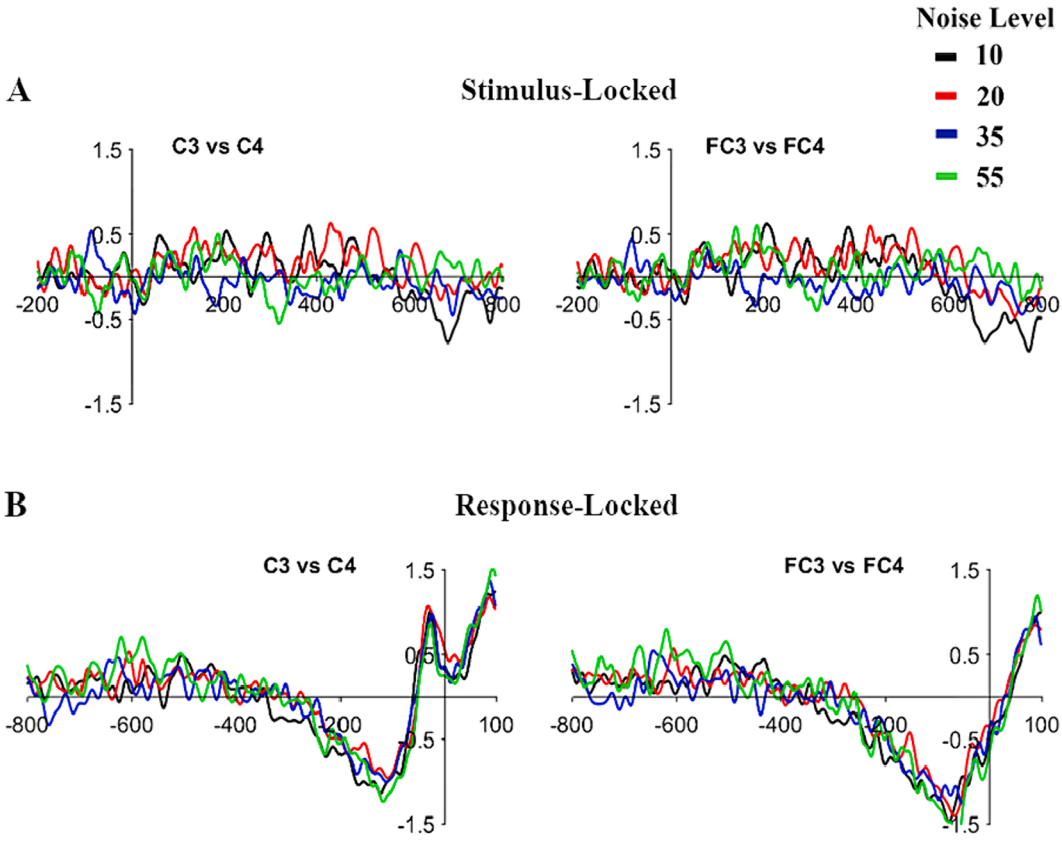

Fig. 4. LRP Results. Stimulus-locked (A) and response-locked (B) LRP activities are shown for two different pairs of electrodes, namely C3 – C4 and FC3 – FC4.

signal distribution was consistent with the previous findings, emphasizing heightened activation in the central brain sites corresponding to the CP1, CP2, and CPz channels, which are the primary focus for CPP. Moreover, the activity in those channels exhibited a pattern of reaching a common level during response irrespective of the task difficulty. These findings bolstered the essential qualities of CPP, highlighting its role in indexing sensory evidence accumulation over time until a certain threshold is attained during the response. Another important implication of the results is the differentiation of motor preparation signal LRP from CPP. It has been found that LRP lagged the CPP formation for approximately 100 to 150 ms. In sum, this study's outcomes resonated with the prior literature, solidifying evidence for a domain-general mechanism driving the perceptual decision-making process.

4.1. Impact on the biological motion perception literature

Previous event-related potential (ERP) studies on biological motion perception have primarily focused on form, motion, and configuration processing, with a particular emphasis on early ERP components, namely N1, P1, as well as N200 and N330 (Hirai et al., 2005; Baccus et al., 2009). Additionally, some studies have delved into higher-level processes involving attention, visual search, and action recognition (White et al., 2014; Hirai & Hiraki, 2006). Notably, a few influential studies have identified a centro-parietal deflection resembling CPP at around 300 ms, suggesting potential involvement in later cognitive processes (Krakowski et al., 2011). To the best of our knowledge, the present study is the first to explicitly investigate perceptual decision-making and related ERPs in the context of biological motion perception. The current study demonstrated the generalizability of the core decision-making mechanisms to biological motion perception tasks.

There is a large body of biological motion literature aiming to understand the effect of underlying low-level features on perception. Local motion, which refers to the kinematics of the individual dots, is found to be crucial for facing direction and animacy detection tasks (Chang and Troje, 2008, Troje and Westhoff, 2006). Yet, the important role of form/structure information arising from the interconnectivity of the individual dots, namely integrative motion (Thirkettle et al., 2009) and opponent motion (Casile & Giese, 2005) have also been emphasized. In this regard, integrating biological motion task into perceptual decision-making framework, that is, investigation of information processing stages in temporally evolving accumulation to bound dynamics derived from EEG signal is promising. Thereby, the study introduced a new approach for future investigations aimed at better understanding the distinct contributions of features and their interactions in biological motion perception, such as global form and local motion.

Furthermore, the findings of the current study, particularly those related to the temporal qualities of the sensory evidence accumulation process, can serve as a potential benchmark for prospective studies. As the application of various dynamic manipulations becomes feasible through PLDs (Decatoire et al., 2019), including the temporal aspects (Thurman & Grossman, 2008) and spatial configurations (Thirkettle et al., 2009), future studies can leverage these advantages to utilize tasks beyond PLD walker direction discrimination. For instance, the potential tasks include action discrimination, biological motion discrimination, or walking direction discrimination task along with a manipulation where the facing and movement direction are distinct. The richness of the manipulations would assist in identifying the specific time intervals and spatial arrangements where task-related information is maximized within the evolving temporal dynamics of the perceptual decision-making framework. Since biological motion perception may not be a single phenomenon, but rather encompassing distinguishable aspects, one can expect to see differences as the outcome of different tasks (Troje, 2008).

Previous studies have also identified relevant brain areas including the posterior superior temporal sulcus (Vaina et al., 2001; Gilaie-Dotan et al., 2013; van Kemenade et al., 2012), and explored the underlying computational aspects through modeling (Giese & Poggio, 2003; Lange & Lappe, 2006; Duarte et al., 2022). One of the most influential models was proposed by Giese and Poggio (2003), suggesting two streams of information processing, namely the ventral and dorsal pathways, that process form and motion, respectively. According to this model, convergence at the superior temporal sulcus integrates these pathways to yield the perception of motion (Giese & Poggio, 2003). There are also other models that have been proposed to explain the global structure-from-motion, local motion processing stages, and infant perceptual abilities (Lange & Lappe, 2006; Hirai & Senju, 2020; Troje, 2008). In this context, another potential impact of the present study is exploring the evolution of the decision process as outlined by the drift–diffusion model parameters (e.g. drift rate, decision threshold, starting point) along with processing the local motion and global form information, which holds the potential for further enhancing our understanding of the mechanisms leading biological motion perception in the brain. Notably, whether the accumulation of evidence occurs through concurrent processing within the two streams or after form-from-motion integration remains to be investigated.

4.2. Impact on the perceptual decision-making literature

The present study introduces a more intricate task involving motion clips, setting it apart from studies that utilize simpler (e.g. RDKs) or static stimuli (e.g. face versus car discrimination) to perceptual decision-making literature. By using PLDs, the advantages over traditionally employed RDKs or other simple/non-static stimuli include increased complexity, social relevance, generalizability of the core decision-making processes, and the variety of questions that can be addressed (e.g. local motion versus global form processing). The important reasons why RDKs are widely preferred in perceptual decision-making studies are their accessibility and ease of manipulation. Similarly, there is an increased accessibility and manipulation techniques in the studies employing PLDs (Lapenta et al., 2017). The variety of manipulations described previously allows adjusting the task difficulty to better understand the task-specific mechanisms and their reflection on the decision-making process. Consequently, the present study extends previous research by employing a more complex and socially relevant task. Furthermore, the results revealed a noteworthy delay in CPP formation compared to previous work employing RDKs (Kelly & O'Connell, 2013), highlighting the responsiveness of perceptual decision-making and CPP to stimulus complexity.

One should note that the domain-general mechanism of perceptual decision-making can manifest through distinct networks. Indeed, the observed variability in latencies for the CPP in the literature during a large interval (300 ms-800 ms), can be attributed to the dynamic interplay between core decision-making brain regions and stimulus-specific ancillary regions. Different cognitive tasks and stimuli may engage these regions to varying extents, resulting in a wide range of observed CPP latencies. Notably, ancillary circuits, that play a complementary role to core decision circuits, may exhibit variations depending on the specific task and stimuli employed. Specifically, in the tasks where accuracy is favored over speed, uncertainty evaluated by prefrontal areas plays a role in the resulting conservative policies which may lead to longer latencies (O'Connell & Kelly, 2021). However, a definitive explanation for this notable range requires further investigation. Future work should focus on disentangling these complex interactions and their impact on CPP timing, potentially revealing more about the underlying cognitive processes. The interactions between stimulus-specific regions leading to decisions deserve further scrutiny. Specifically, the role of pSTS merits deeper exploration using a similar paradigm, as this region has been linked with biological motion perception (Saygin et al., 2004), and is considered to be a convergence point for dorsal and ventral pathways (Giese & Poggio, 2003). Additionally, studying the network connecting pSTS and homologous parietal regions in humans to macaque LIP holds promise, akin to research

exploring differences between the neural responses of MT and LIP regions (Gold & Shadlen, 2007).

Investigating the parameters influenced by stimulus characteristics resulting in a later rise in CPP in the present study is also an avenue worth exploring. The recent models incorporate concepts such as drift rate, speed-accuracy trade-offs, urgency signals, and uncertainty signals (O'Connell & Kelly, 2021; Hanks & Summerfield, 2017). Likewise, studying these processes gains more significance when considering biological motion stimuli, given their potential to reflect evolutionarily and socially meaningful scenarios. Concurrently, models of perceptual decision-making stand to benefit from incorporating biological motion tasks.

4.3. Limitations and future research

The present study bears its first limitation concerning the stimuli used. Although temporal qualities of scrambled motion are manipulated by varying the display time, there are also other potential manipulations. Importantly, it would be worth exploring the manipulation of the speed of the stimuli used in the task. Such an investigation could alter the CPP onset and latency, revealing potential nonlinear effects of speed on the sensory evidence accumulation process. In addition, point-light displays, while effective in capturing crucial aspects of biological motion, could be complemented by more naturalistic videos depicting human actions or even real human actors in naturalistic settings. This avenue of research aligns with the growing adoption of real-time EEG methodologies, offering the opportunity to enhance ecological validity (Stangl et al., 2023; Pekçetin et al., 2023).

Another limitation of the study comes from the task being employed. The current study included explicit instructions for participants to report the walking direction upon recognizing a human figure. This was emphasized to ensure that responses were based on the perception of human gait patterns rather than isolated local movements. Additionally, participants were familiarized with the task in a pre-experimental session to minimize misunderstandings about the task requirements. Despite these, we acknowledge the possibility that subjects might rely primarily on local motion trajectories as demonstrated previously even in the absence of structural configuration for reporting the walking direction (Troje & Westhoff, 2006). Future work employing a detection or action discrimination rather than a direction task would be valuable in ensuring global form processing. Additionally, employing "moonwalker" stimuli is also possible to differentiate the global versus local processing when the facing and movement direction are distinct (Miller & Saygin, 2013).

It should also be noted that the current study would benefit from explicit investigations of whether CPP observed with respect to our task indeed reflects the two essential components of the drift–diffusion model. Recent endeavors in computational modeling, notably neurally informed models, extend beyond traditional drift–diffusion models while explaining more complex mechanisms. The researchers benefit from CPP and mu/beta activity for informing, i.e. constraining the model parameters, which aligns with this study's approach (Kelly et al., 2021). With the inclusion of time constraints and speed-accuracy trade-offs, these models offer a promising direction for future investigations. The endeavors encompassing the above-mentioned models will also help disentangle the underlying processes for the evidence accumulation within the biological motion perception task in comparison to largely employed random dot kinematics. In this context, further research is planned by also incorporating different aspects of perceptual decision-making (e.g. prior information, feedback, speed-accuracy trade-off, etc.) which is for the time being, beyond the scope of this paper.

Lastly, while the task employed in the present study focused on visual perception, the integration of sensory information holds great significance in our daily experiences. This also holds for biological motion perception in natural settings since it consists of and requires multisensory input (Brooks et al., 2007). Despite the prevailing use of visual motion displays, the exploration of audio-visual cues for human motion in natural settings is a growing area of research (Mendonça et al., 2011). Therefore, it would be worth investigating the effects of multisensory integration on the CPP build-up using a similar experiment. Anticipated benefits of multimodal integration include more efficient sensory evidence accumulation which may potentially lead to earlier latencies and heightened peaks in CPP.

5. Conclusion

In conclusion, the present study extends our understanding of perceptual decision-making by demonstrating domain-general mechanisms within the context of a biological motion direction discrimination task. The introduction of PLDs to the field offers significant advantages over traditionally employed RDKs. The integration of perceptual decision-making and biological motion perception holds promise for further studies. Through employing different tasks (e.g. action recognition, detection), the underlying mechanisms of local and global processes in biological motion perception along with the decision variables can be investigated in future research.

6. Ethics statement

The participants in the present study completed written informed consent form prior to the experimental session. The study approved by the Human Research Ethics Board of Bilkent University and adheres to the ethical principles outlined in the Declaration of Helsinki.

CRediT authorship contribution statement

Osman Cagri Oguz: Writing – original draft, Visualization, Software, Methodology, Formal analysis. **Berfin Aydin:** Software, Data curation, Conceptualization. **Burcu A. Urgen:** Writing – review & editing, Supervision, Project administration, Methodology, Conceptualization.

Data availability

Data from this study will be made available on the Open Science Framework (https://osf.io/gbn2r/) after publication of the study, as far as data protection regulations permit.

Data and codes used from the present study will be made available on the Open Science Framework (https://osf.io/5vb6k/) following the publication of the study.

Appendix A. Supplementary data

Supplementary data to this article can be found online at https://doi.org/10.1016/j.visres.2024.108380.

References

Bach, D. R., Pryce, C. R., & Seifritz, E. (2011). The experimental manipulation of uncertainty. In J. Raber (Ed.), *Animal Models of Behavioral Analysis* (pp. 193–216). Totowa, NJ: Springer Press.

Baccus, W., Mozgova, O., & Thompson, J. C. (2009). Early integration of form and motion in the neural response to biological motion. *Neuroreport, 20*(15), 1334–1338. https://doi.org/10.1097/WNR.0b013e328330a867

Blake, R., & Shiffrar, M. (2007). Perception of human motion. *Annual Review of Psychology, 58*, 47–73. https://doi.org/10.1146/annurev.psych.57.102904.190152

Brooks, A., van der Zwan, R., Billard, A., Petreska, B., Clarke, S., & Blanke, O. (2007). Auditory motion affects visual biological motion processing. *Neuropsychologia, 45*(3), 523–530.

Casile, A., & Giese, M. A. (2005). Critical features for the recognition of biological motion. *Journal of Vision, 5*(4), 348–360. https://doi.org/10.1167/5.4.6

Chang, D. H., & Troje, N. F. (2008). Perception of animacy and direction from local biological motion signals. *Journal of Vision, 8*(5), 1–10. https://doi.org/10.1167/8.5.3

Cheadle, S., Wyart, V., Tsetsos, K., Myers, N., de Gardelle, V., Herce Castañón, S., & Summerfield, C. (2014). Adaptive gain control during human perceptual choice. *Neuron, 81*(6), 1429–1441. https://doi.org/10.1016/j.neuron.2014.01.020

de Lange, F. P., Jensen, O., & Dehaene, S. (2010). Accumulation of evidence during sequential decision making: The importance of top-down factors. *Journal of Neuroscience, 30*, 731–738.

Decatoire, A., Beauprez, S. A., Pylouster, J., Lacouture, P., Blandin, Y., & Bidet-Ildei, C. (2019). PLAViMoP: How to standardize and simplify the use of point-light displays. *Behavior Research Methods, 51*(6), 2573–2596. https://doi.org/10.3758/s13428-018-1112-x

de Jong, R., Wierda, M., Mulder, G., & Mulder, L. J. (1988). Use of partial stimulus information in response processing. *Journal of Experimental Psychology: Human Perception and Performance, 14*(4), 682–692. https://doi.org/10.1037/0096-1523.14.4.682

Delorme, A., & Makeig, S. (2004). EEGLAB: An open-source toolbox for analysis of single-trial EEG dynamics including independent component analysis. *Journal of Neuroscience Methods, 134*, 9–21.

Duarte, J. V., Abreu, R., & Castelo-Branco, M. (2022). A two-stage framework for neural processing of biological motion. *NeuroImage, 259*, Article 119403. https://doi.org/10.1016/j.neuroimage.2022.119403

Eimer, M. (1998). The lateralized readiness potential as an on-line measure of central response activation processes. *Behavior Research Methods, Instruments, & Computers, 30*, 146–156. https://doi.org/10.3758/BF03209424

Fields, E. C. (2017). Factorial Mass Univariate ERP Toolbox [Computer software]. Available from: https://github.com/ericcfields/FMUT/releases.

Fields, E. C., & Kuperberg, G. R. (2020). Having your cake and eating it too: Flexibility and power with mass univariate statistics for ERP data. *Psychophysiology, 57*(2), e13468.

Giese, M. A., & Poggio, T. (2003). Neural mechanisms for the recognition of biological movements. *Nature Reviews. Neuroscience, 4*(3), 179–192. https://doi.org/10.1038/nrn1057

Gilaie-Dotan, S., Kanai, R., Bahrami, B., Rees, G., & Saygin, A. P. (2013). Neuroanatomical correlates of biological motion detection. *Neuropsychologia, 51*(3), 457–463. https://doi.org/10.1016/j.neuropsychologia.2012.11.027

Gratton, G., Coles, M. G., Sirevaag, E. J., Eriksen, C. W., & Donchin, E. (1988). Pre- and post-stimulus activation of response channels: A psychophysiological analysis. *Journal of Experimental Psychology: Human Perception and Performance, 14*, 331–344.

Gold, J. I., & Shadlen, M. N. (2007). The neural basis of decision making. *Annual Review of Neuroscience, 30*, 535–574. https://doi.org/10.1146/annurev.neuro.29.051605.113038

Gorea, A., Belkoura, S., & Solomon, J. A. (2014). Summary statistics for size over space and time. *Journal of Vision, 14*(9), 22. https://doi.org/10.1167/14.9.22

Hanks, T. D., & Summerfield, C. (2017). Perceptual decision making in rodents, monkeys, and humans. *Neuron, 93*(1), 15–31. https://doi.org/10.1016/j.neuron.2016.12.003

Heekeren, H. R., Marrett, S., & Ungerleider, L. G. (2008). The neural systems that mediate human perceptual decision-making. *Nature Reviews Neuroscience., 9*, 467–479.

Herding, J., Ludwig, S., von Lautz, A., Spitzer, B., & Blankenburg, F. (2019). Centro-parietal EEG potentials index subjective evidence and confidence during perceptual decision making. *NeuroImage, 201*, Article 116011. https://doi.org/10.1016/j.neuroimage.2019.116011

Hirai, M., & Hiraki, K. (2006). Visual search for biological motion: An event-related potential study. *Neuroscience Letters, 403*(3), 299–304. https://doi.org/10.1016/j.neulet.2006.05.002

Hirai, M., & Senju, A. (2020). The two-process theory of biological motion processing. *Neuroscience and Biobehavioral Reviews, 111*, 114–124. https://doi.org/10.1016/j.neubiorev.2020.01.010

Hirai, M., Senju, A., Fukushima, H., & Hiraki, K. (2005). Active processing of biological motion perception: An ERP study. *Brain Research. Cognitive Brain Research, 23*(2–3), 387–396. https://doi.org/10.1016/j.cogbrainres.2004.11.005

Horwitz, G. D., & Newsome, W. T. (1999). Separate signals for target selection and movement specification in the superior colliculus. *Science (New York, N.Y.), 284*(5417), 1158–1161. https://doi.org/10.1126/science.284.5417.1158

Johansson, G. (1973). Visual perception of biological motion and a model for its analysis. *Perception & Psychophysics, 14*, 201–211.

Johansson, G. (1976). Spatio-temporal differentiation and integration in visual motion perception. *Psychological Research, 38*, 379–393.

Johnson, K. L., & Shiffrar, M. (Eds.). (2013). *People watching: Social, perceptual, and neurophysiological studies of body perception*. Oxford University Press.

Kaiser, J., Lennert, T., & Lutzenberger, W. (2006). Dynamics of oscillatory activity during auditory decision making. *Cerebral Cortex, 17*, 2258–2267.

Kelly, S. P., Corbett, E. A., & O'Connell, R. G. (2021). Neurocomputational mechanisms of prior-informed perceptual decision-making in humans. *Nature Human Behaviour, 5*(4), 467–481.

Kelly, S. P., & O'Connell, R. G. (2013). Internal and external influences on the rate of sensory evidence accumulation in the human brain. *Journal of Neuroscience, 33*(50), 19434–19441.

Kelly, S. P., & O'Connell, R. G. (2015). The neural processes underlying perceptual decision making in humans: Recent progress and future directions. *Journal of Physiology-Paris, 109*(1–3), 27–37.

Kim, J. N., & Shadlen, M. (1999). Neural correlates of a decision in the dorsolateral prefrontal cortex of the macaque. *Nature Neuroscience, 2*, 176–185. https://doi.org/10.1038/5739

Krakowski, A. I., Ross, L. A., Snyder, A. C., Sehatpour, P., Kelly, S. P., & Foxe, J. J. (2011). The neurophysiology of human biological motion processing: A high-density electrical mapping study. *NeuroImage, 56*(1), 373–383. https://doi.org/10.1016/j.neuroimage.2011.01.058

Lange, J., & Lappe, M. (2006). A model of biological motion perception from configural form cues. *The Journal of Neuroscience, 26*(11), 2894–2906. https://doi.org/10.1523/JNEUROSCI.4915-05.2006

Lapenta, O. M., Xavier, A. P., Còrrea, S. C., et al. (2017). Human biological and nonbiological point-light movements: Creation and validation of the dataset. *Behavioral Research, 49*, 2083–2092. https://doi.org/10.3758/s13428-016-0843-9

Lopez-Calderon, J., & Luck, S. J. (2014). ERPLAB: An open-source toolbox for the analysis of event-related potentials. *Frontiers in Human Neuroscience, 8*, 213.

Lui, K. K., Nunez, M. D., Cassidy, J. M., Vandekerckhove, J., Cramer, S. C., & Srinivasan, R. (2021). Timing of readiness potentials reflect a decision-making process in the human brain. *Computational Brain & Behavior, 4*(3), 264–283. https://doi.org/10.1007/s42113-020-00097-5

Mendonça, C., Santos, J. A., & López-Moliner, J. (2011). The benefit of multisensory integration with biological motion signals. *Experimental Brain Research, 213*(2–3), 185–192. https://doi.org/10.1007/s00221-011-2620-4

Miller, L. E., & Saygin, A. P. (2013). Individual differences in the perception of biological motion: Links to social cognition and motor imagery. *Cognition, 128*(2), 140–148. https://doi.org/10.1016/j.cognition.2013.03.013

Newsome, W. T., Britten, K. H., & Movshon, J. A. (1989). Neuronal correlates of a perceptual decision. *Nature, 341*, 52–54.

O'Connell, R., Dockree, P., & Kelly, S. (2012). A supramodal accumulation-to-bound signal that determines perceptual decisions in humans. *Nature Neuroscience, 15*, 1729–1735. https://doi.org/10.1038/nn.3248

O'Connell, R. G., & Kelly, S. P. (2021). Neurophysiology of human perceptual decision-making. *Annual Review of Neuroscience, 44*, 495–516. https://doi.org/10.1146/annurev-neuro-092019-100200

Pavlova, M. A. (2012). Biological motion processing as a hallmark of social cognition. *Cerebral Cortex, 22*(5), 981–995. https://doi.org/10.1093/cercor/bhr156

Pekçetin, T. N., Evsen, Ş., Pekçetin, S., Acarturk, C., & Urgen, B. A. (2023). A naturalistic setup for presenting real people and live actions in experimental psychology and cognitive neuroscience studies. *Journal of Visualized Experiments, 198*, e65436.

Philiastides, M. G., Ratcliff, R., & Sajda, P. (2006). Neural representation of task difficulty and decision making during perceptual categorization: A timing diagram. *Journal of Neuroscience, 26*, 8965–8975.

Philiastides, M. G., & Sajda, P. (2006). Temporal characterization of the neural correlates of perceptual decision making in the human brain. *Cerebral Cortex, 16*(4), 509–518. https://doi.org/10.1093/cercor/bhi130

Ratcliff, R., & McKoon, G. (2008). The diffusion decision model: Theory and data for two-choice decision tasks. *Neural Computation, 20*(4), 873–922. https://doi.org/10.1162/neco.2008.12-06-420

Rutherford, M. D., & Kuhlmeier, V. A. (2013). Social perception: Detection and interpretation of animacy, agency, and intention. *Boston Review*. https://doi.org/10.7551/mitpress/9780262019279.001.0001

Saygin, A. P., Wilson, S. M., Hagler, D. J., Jr, & Sereno, M. I. (2004). Point-light biological motion perception activates human premotor cortex. *The Journal of Neuroscience: the official journal of the Society for Neuroscience, 24*(27), 6181–6188. https://doi.org/10.1523/JNEUROSCI.0504-04.2004

Shadlen, M. N., & Newsome, W. T. (1996). Motion perception: Seeing and deciding. *Proceedings of the National Academy of Sciences of the United States of America, 93*(2), 628–633. https://doi.org/10.1073/pnas.93.2.628

Shadlen, M. N., & Newsome, W. T. (2001). Neural basis of a perceptual decision in the parietal cortex (area LIP) of the rhesus monkey. *Journal of Neurophysiology, 86*(4), 1916–1936. https://doi.org/10.1152/jn.2001.86.4.1916

Smith, P. L., & Ratcliff, R. (2004). A comparison of sequential sampling models for two-choice reaction time. *Psychological Review, 111*(2), 333–367. https://doi.org/10.1037/0033-295X.111.2.333

Smulders, F. T. Y., & Miller, J. O. (2012). The lateralized readiness potential. In S. J. Luck, & E. S. Kappenman (Eds.), *The Oxford handbook of event-related potential components* (pp. 209–229). Oxford University Press.

Stangl, M., Maoz, S. L., & Suthana, N. (2023). Mobile cognition: Imaging the human brain in the 'real world'. *Nature Reviews. Neuroscience, 24*(6), 347–362. https://doi.org/10.1038/s41583-023-00692-y

Thirkettle, M., Benton, C. P., & Scott-Samuel, N. E. (2009). Contributions of form, motion and task to biological motion perception. *Journal of Vision, 9*(3), 1–11.

Thornton, I. M. (2006). *Biological motion: Point-light walkers and beyond.in human body perception from the inside out: Advances in visual cognition* (pp. 271–303). Oxford University Press.

Troje, N. F., & Westhoff, C. (2006). The inversion effect in biological motion perception: Evidence for a "life detector?". *Current Biology: CB, 16*(8), 821–824. https://doi.org/10.1016/j.cub.2006.03.022

Troje, N. F. (2008). Biological motion perception. Vision II. In A. Basbaum, A. Kaneko, G. M. Shepherd, & G. Westheimer (Eds.), *The senses: A comprehensive reference* (pp. 231–238). Elsevier. Crossref.

Thurman, S. M., & Grossman, E. D. (2008). Temporal "bubbles" reveal key features for point-light biological motion perception. *Journal of Vision, 8*(3), 1–11. https://doi.org/10.1167/8.3.28

Twomey, D. M., Murphy, P. R., Kelly, S. P., & O'Connell, R. G. (2015). The classic P300 encodes a build-to-threshold decision variable. *European Journal of Neuroscience, 42*, 1636–1643. https://doi.org/10.1111/ejn.12936

Vaina, L. M., Solomon, J., Chowdhury, S., Sinha, P., & Belliveau, J. W. (2001). Functional neuroanatomy of biological motion perception in humans. *Proceedings of the National*

Academy of Sciences of the United States of America, 98(20), 11656–11661. https://doi.org/10.1073/pnas.191374198

van Kemenade, B. M., Muggleton, N., Walsh, V., & Saygin, A. P. (2012). Effects of TMS over premotor and superior temporal cortices on biological motion perception. *Journal of cognitive neuroscience, 24*(4), 896–904. https://doi.org/10.1162/jocn_a_00194

White, N. C., Fawcett, J. M., & Newman, A. J. (2014). Electrophysiological markers of biological motion and human form recognition. *NeuroImage, 84*, 854–867. https://doi.org/10.1016/j.neuroimage.2013.09.026